Quantifying Volume Reduction and Peak Flow Mitigation for Three Bioretention Cells in Clay Soils in Northeast Ohio

Ryan J. Winston, PhD, P.E.[a], Jay D. Dorsey, PhD, P.E.[b], and William F. Hunt, PhD, P.E.[c]

[a]Presently: Research Scientist, Department of Food, Agricultural, and Biological Engineering, the Ohio State University, USA. Formerly: PhD Candidate, Department of Biological and Agricultural Engineering, North Carolina State University, Campus Box 7625, Raleigh, NC, USA 27695. Phone: (919) 515-8595. Fax: (919) 515-6772. rjwinsto@gmail.com. Corresponding author.

[b]Water Resources Engineer, Ohio Department of Natural Resources, Division of Soil and Water Resources, 2045 Morse Road, Building B-3, Columbus, Ohio, USA 43299. Jay.Dorsey@epa.ohio.gov

[c]William Neal Reynolds Professor and Extension Specialist, Department of Biological and Agricultural Engineering, North Carolina State University, Campus Box 7625, Raleigh, NC, USA 27695. wfhunt@ncsu.edu

Abstract

Green infrastructure aims to restore watershed hydrologic function by more closely mimicking pre-development groundwater recharge and evapotranspiration (ET). Bioretention has become a popular stormwater control due to its ability to reduce runoff volume through these pathways. Three bioretention cells constructed in low permeability soils in northeast Ohio were monitored for non-winter quantification of inflow, drainage, ET, and exfiltration. The inclusion of an internal water storage (IWS) zone allowed the three cells to reduce runoff 59%, 42%, and 36% over the monitoring period, in spite of the tight underlying soils. The exfiltration rate and the IWS zone thickness were the primary determinants of volume reduction performance. Post-construction measured drawdown rates were *higher* than pre-construction soil vertical hydraulic conductivity tests in all cases, due to lateral exfiltration from the IWS zones and ET, which are not typically accounted for in pre-construction soil testing. The minimum rainfall depths required to produce outflow for the three cells were 5.5, 7.4, and 13.8 mm. During events with 1-year design rainfall intensities, peak flow reduction varied from 24 to 96%, with the best mitigation during events where peak rainfall rate occurred before the centroid of the rainfall volume, when adequate bowl storage was available to limit overflow.

Keywords

Biofilter; exfiltration; internal water storage; hydrology; hydraulics; flow duration

1 Introduction

Urban development generates impervious surfaces and soil compaction, modifying the hydrological cycle by reducing infiltration and evapotranspiration (ET) while increasing surface

runoff (Bledsoe and Watson 2001; Booth et al. 2002; Walsh et al. 2012; Chen et al. 2014). Watershed imperviousness of 10% or more has been shown to negatively impact stream ecology, habitat, and water quality (Wang et al. 2001; Schueler et al. 2009). Incision and bank erosion caused cross-sectional area of urban streams to be 3.8 times larger than rural streams in Piedmont Pennsylvania (Hammer 1972; Booth 1990).

Low Impact Development (LID) technologies, such as bioretention (also termed biofilters), are purported to more closely mimic pre-development hydrology, including duration, rate, and volume of flow (PGC 2001; USEPA 2007; Cizek and Hunt 2013; Page et al. 2015a). DeBusk et al. (2011) found drainage from bioretention cells was released at rates similar to shallow interflow in rural reference watersheds, suggesting watershed scale implementation of bioretention could benefit stream health through disconnection of imperviousness (Walsh et al. 2009; Burns et al. 2012). Runoff volume reduction provided by bioretention cells improves water quality by substantially reducing pollutant loading to surface water bodies, lessening stream erosion rates, recharging groundwater and providing baseflow to urban streams, and helping to reduce the water quality impacts of combined sewer overflows (Tillinghast et al. 2012; Hamel et al. 2015; Autixier et al. 2014; Lucas and Sample 2015). In contract, recent studies have shown detention basins may amplify the duration of critical erosion-causing discharges, furthering stream degradation (Palhegyi 2009; Tillinghast et al. 2011).

Bioretention cells are biologically-based media filters designed to temporarily store and treat a prescribed water quality volume (e.g., runoff from a 19-mm wet weather event in Ohio) from highly impervious catchments (ODNR 2006). Typically, bioretention cells pond 22-30 cm of stormwater in their surface storage (i.e., bowl), have 60-120 cm of bioretention media and, when underlying soils are poorly drained, have an underdrain surrounded by a gravel layer to allow for

inter-event drainage (Davis 2008; Li et al. 2009; Davis et al. 2009; Figure 1). Once the bowl fills, a bypass or overflow structure conveys flow to the storm or combined sewer network.

Bioretention media is a mixture of sand (usually the vast majority of the media), fines (silt and clay), and organic matter, with 5-10 cm/hr typically targeted as a design infiltration rate (Dietz and Clausen 2005; Emerson and Traver 2008; Hunt et al. 2012). The media supports the growth of plants, typically trees, shrubs, forbs, and/or grasses chosen for their ability to withstand primarily droughty but also temporarily inundated conditions (Bratieres et al. 2008; Page et al. 2015b). Vegetation promotes ET and maintains the soil infiltration rate over time, with root macropores appearing to offset the negative effects of media compaction and sediment deposition (Jenkins et al. 2010).

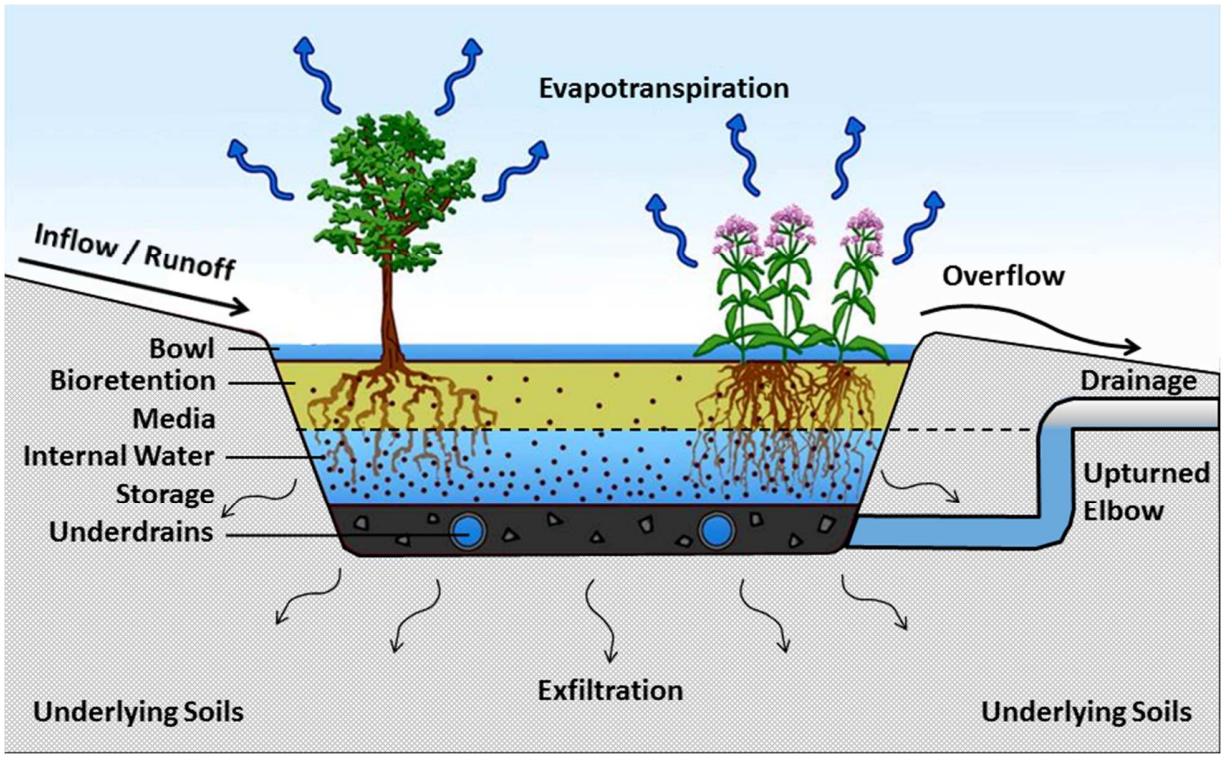

Figure 1. Schematic of a bioretention cell with an internal water storage (IWS) zone (courtesy Shawn Kennedy, NCSU)

Four pathways exist for outflow from bioretention cells: exfiltration to the underlying soil, ET, drainage through the underdrain, and overflow/bypass. Bioretention cells often capture in their entirety (and do not release runoff from) storms smaller than the water quality design storm (Davis 2008; Hunt et al. 2008; Li et al. 2009; Jones and Hunt 2009), which translates into substantial abstraction of long-term runoff volume (Davis, Traver et al. 2012). For instance, 18% of events monitored at two bioretention facilities in Maryland which were lined with an impermeable membrane had no outflow (Davis 2008). Thirty-three percent of the inflow volume was retained in lined biofilters in Australia, with retention proportional to rainfall depth (Hatt et al. 2009). Luell (2011) studied two bioretention cells built in compacted sandy clay loam soils, one sized to treat the 25-mm event and one to treat the 12.5-mm event. The cells reduced runoff volume by 30% and 20%, respectively. Deeper media depths promoted additional exfiltration (Brown and Hunt 2011a). Exfiltration and ET resulted in 50-90% volume reduction from bioretention facilities (Heasom et al. 2006; Hunt et al. 2006), and was dependent on the underlying soil type. Li et al. (2009) showed ET was 15-20% of inflow for a bioretention cell in Louisburg, NC.

Peak flow mitigation in a bioretention cell was directly associated with its surface area, surface storage volume, the infiltration rate of the media, and the exfiltration rate (Davis et al. 2009; Davis, Traver et al. 2012). Peak flow mitigation was 65% in Connecticut (Dietz and Clausen 2005), 80-90% in Australia (Hatt et al. 2009; Lucke and Nichols 2015), and seasonally variable but lower in winter (Muthanna et al. 2008). To maximize peak flow mitigation, proportionally large bioretention surface area and deeper media depth are desired (Li et al. 2009; Davis, Traver et al. 2012).

The underdrain configuration in a bioretention cell substantially impacts volume reduction (Brown and Hunt 2011b); it may lack an underdrain when underlying soils are highly transmissive, employ an underdrain at the bottom of the cross-section, have an underdrain with a valve or orifice to control outflow rate (City of Omaha 2014; MPCA 2015; Guo and Luu 2015), or utilize an internal water storage zone (IWS). An IWS zone is created by an upturned elbow in the underdrain, forcing internal ponding within the media (Figure 1). The IWS zone is typically 0.3 to 0.75-m deep (Hunt et al., 2006; Passeport et al., 2009). With low permeability underlying soils, the IWS zone will dewater slowly. In these conditions, a zone of aerobic media should be maintained above the IWS zone for plant growth and to prevent leaching of heavy metals (Blecken et al. 2009). The IWS zone was originally recommended to promote denitrification (Hunt et al. 2006; Dietz and Clausen 2006; Davis 2008; Passeport et al. 2009), but has been shown to substantially improve volume reduction (Dietz and Clausen 2006; Brown and Hunt 2011b; Winston 2016). Li et al. (2009) reported a bioretention cell with an IWS zone produced outflow during 37% of observed storms, while a neighboring, otherwise identical, cell with no IWS zone had outflow for 65% of storms. The mechanism for augmented volume reduction was the additional storage provided by inter-event exfiltration, which otherwise is limited in bioretention cells.

While bioretention design has been informed through synthesized research studies (e.g., Hunt et al. 2012), the hydrology of bioretention systems over poorly drained soils has not been thoroughly documented in the field to-date. These infiltration-based stormwater control measures (SCMs) are often specified in Hydrologic Soil Group (HSG) A and B soils, with some entities discouraging their use in poorly drained soils (IDNR 2010). The goal of this study was

to quantify bioretention hydrologic performance with an IWS zone and when built in HSG D soils. Three bioretention cells in northeastern Ohio were examined.

2 Site Descriptions

The water balance was determined on a storm-by-storm basis for two bioretention cells at Holden Arboretum (HA) and one at Ursuline College (UC; Figure 2). Design guidance in the *Ohio Rainwater and Land Development Manual* (ODNR 2006) requires a bioretention cell to capture the 19-mm water quality volume in its bowl and have a filter bed surface area of 5% of the impervious contributing catchment. All three bioretention cells were located in areas with mapped HSG D soils according to the Ohio soil survey [Platea and Pierpont silty clay loam (HA) and Mahoning silt loam (UC), Soil Survey Staff (2015)].

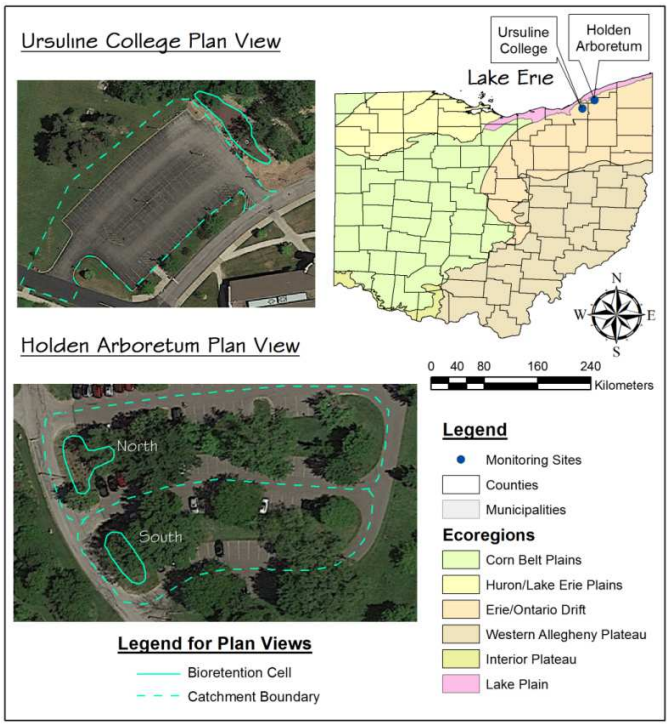

Figure 2. Location of bioretention facilities in northeast Ohio.

A bioretention cell was constructed during April-May of 2014 on the campus of UC to treat a 0.36 ha, 77.1% impervious catchment consisting of a parking lot and peripheral pervious areas (Table 1 and Figure 3). The filter bed surface area was 182 m^2 (6.5% of the contributing impervious catchment). The surveyed bowl depth was 30 cm, and water ponding above this level overflowed through the catch basin (Figure 3). Surface (i.e., bowl) storage volume was 60 m^3, compared to the water quality volume of 39 m^3; therefore, this bioretention cell was oversized and stored the runoff from a 29.5-mm storm event in its bowl (Table 1).

Figure 3. The UC (left) bioretention cell six months post-construction and the HA South (middle) and North (right) bioretention cells 13 months post-construction.

Table 1. Summary of bioretention cell and catchment characteristics.

Characteristics	UC	HA South	HA North
Catchment area (m^2)	3600	1900	2700
Catchment percent imperviousness	77	58	58
Bioretention surface area (m^2)	182	57	79
Surface storage volume (m^3)	60	35	48
As-built design event (mm)	29.5	45.2	44.7
Average bowl storage depth (m)	0.30	0.39	0.40
Mulch layer thickness (m)	0.08	0.08	0.08
Fill media depth (m)	0.60	0.84	0.90
Gravel layer thickness (m)	0.30	0.30	0.30
Choking stone + sand layer thickness (m)	0.15	0.15	0.15
IWS zone thickness (m)	0.60	0.38	0.45
Underdrain diameter (cm)	15	10	10
Media characteristics[1]	87% sand, 4% silt, 9% clay	88% sand, 2% silt, 10% clay	88% sand, 2% silt, 10% clay
Media percent organic matter (by weight)[2]	4.3%	1.4%	1.0%

Media textural classification	Loamy sand	Loamy sand	Loamy sand
Media saturated hydraulic conductivity	168 mm/hr[3]	100 mm/hr	100 mm/hr
Vegetation	Forbs and perennial grasses	Forbs and perennial grasses	Shrubs/trees

[1]determined using sieve methods (ASTM 2007)

[2]determined using loss-on-ignition methods (ASTM 2014)

[3]determined using constant head permeability test using methods in Klute (1986) on triplicate 75 mm soil cores taken from the top 0.3 m of media

The bioretention media was 87% sand, 4% silt, and 9% clay, resulting in a loamy sand soil texture (Table 1). Organic matter was 4.3% of the media by mass. The media was 0.6-m deep and was underlain by 7.5 cm of medium coarse sand, 7.5 cm of pea gravel (1.2-12.7 mm nominal diameter), and 30 cm of #57 aggregate (4.8-25 mm nominal diameter; ASTM 2012). A single 15-cm diameter underdrain drained the cell, and a 60-cm deep IWS zone extended through the gravel and sand layers and 15 cm into the bioretention media. Forty-five cm of media was located above the underdrain invert. The bioretention cell was planted with 1450 plugs [see Winston et al. (2015) for plant list], and a 7.5-cm layer of hardwood mulch was spread over the media. During the monitoring period, the plants were juvenile and developed shoots less than 30 cm tall; therefore, plant processes were not expected to play a major role in the hydrologic results of this study at UC.

Two bioretention cells were constructed at HA in September 2013 (Table 1 and Figure 3). HA South and North had catchment areas of 0.19 and 0.27 ha, respectively (Figure 2). Forty-two percent of each catchment was pervious and well vegetated with turfgrass and mature trees. Filter bed surface areas for HA South and North were 57 and 79 m^2, respectively; these values represented 5% of their respective impervious catchment areas. The HA South and North cells were built with 39 and 40-cm (instead of the intended 30 cm) ponding depths due to a miscommunication during construction (Table 1). The resulting surface storage volume of HA

South was 35 m^3, compared with the water quality volume of 14.6 m^3; therefore, the bioretention cell was actually sized for the 45.2-mm storm event. For HA North, as-built surface storage was 48 m^3, considerably more than the 20.4 m^3 water quality volume. It was sized to capture the 44.7-mm event without overflow.

Media depths were 84 cm for HA South and 90 cm for HA North. The media was 88% sand, 2% silt, and 10% clay and contained 1.4% and 1.0% organic matter by weight for HA South and North, respectively. The media was underlain by 7.5 cm of coarse sand, 7.5 cm of pea gravel, and 30 cm of #57 aggregate. Hardwood mulch (7.5 cm depth) was spread over the media. Underdrains were 10 cm in diameter and were tied into existing catch basins located within each cell. IWS zones of 38- and 45-cm were incorporated into the HA South and North cells, respectively. The HA cells were planted with a mixture of 26 shrubs and one tree (woody plants) in the North cell and 172 forb and perennial grass varieties (herbaceous species) in the South cell (Winston et al. 2015).

3 Materials and Methods

3.1 Data Collection

A weather station (Hobo, Onset Computer Corporation, Bourne, MA) was deployed at each site to measure wind speed, wind direction, air temperature, relative humidity, and solar radiation. Rainfall was measured at each site using a 0.254-mm resolution tipping-bucket rain gauge (Davis Instruments, Hayward, California). Rainfall data were stored in the data logger in the adjacent weather station. Rain gauges and weather stations were located in areas free from obstructions. All climatic parameters were recorded on a 1-minute interval.

Combined overflow and drainage from each bioretention cell was monitored using a sharp crested, v-notch weir and a Hobo U20 pressure transducer (Onset Computer Corporation, Bourne, MA). The pressure transducer was placed immediately downstream of an internal baffle, as far upstream from the weir as possible. Forty-five degree (HA North) or 60˚ (UC and HA South) v-notch weirs were employed depending on the expected flow rates from the bioretention cells. Internal water level (stage) in the bioretention media was measured using a Hobo U20 pressure transducer within a perforated PVC well. Since the pressure transducers were non-vented, an additional U20 pressure transducer was placed in the rain gauge housing at each site to measure (and later correct for) local barometric pressure using a pressure correction algorithm built into the Hoboware software. Pressure transducers recorded data on a 2-minute interval and were downloaded every 3 weeks.

3.2 Data Analysis

Summary statistics were developed for rainfall depth (mm), average rainfall intensity (mm/hr), peak 5-minute rainfall intensity (mm/hr), and antecedent dry period (ADP, days). Discrete storm events were identified by a minimum ADP of 6 hours and rainfall depth of 2.5 mm.

The use of a weir or flume to measure inflow was precluded by diffuse inflow to each bioretention cell. Inflow was determined using a rainfall-runoff model, the NRCS curve number method (USDA-NRCS 1986):

$$Q = \frac{(P-0.2S)^2}{(P+0.8S)} \times \frac{A}{1000} \quad (1)$$

where Q is runoff volume (m^3), P is precipitation depth (mm), S is potential maximum soil moisture retention (mm) and is equal to $(\frac{1000}{CN} - 10) \times 25.4$, CN = curve number for the catchment, and A is the surface area of the catchment (m^2).

Inflow volumes were calculated for each runoff producing event (i.e., $P > 0.2 \times S$). Impervious areas within each catchment were assigned the standard CN of 98 (i.e., almost all rainfall becomes runoff), while pervious areas were assigned a CN of 80 for open space in good condition (>75% grass cover) on an HSG D soil (Fangmeier et al. 2006). Discrete runoff volumes for permeable and impermeable catchment areas were calculated separately and summed, as suggested in Chin (2006). Corrections were applied to the CN for dry and wet antecedent moisture conditions (USDA-NRCS 2004). Antecedent dry periods less than 2 and greater than 5 days were considered wet and dry, respectively. While some error is present due to the use of this method (especially for events less than 12 mm), these smaller events were typically completely captured (i.e. no outflow), resulting in zero discharge from the cells.

Peak inflow rates were calculated using the Rational Method (Chin 2006), which relates rainfall intensity to flow rate:

$$Q_p = 2.78 \times C \times i \times A \quad (2)$$

where Q_p is the peak flow rate (L/s), C is the Rational runoff coefficient, i is the peak 5-minute rainfall intensity (mm/hr), and A is the catchment area (ha). The rational coefficient is customarily 0.9 for impervious areas, while pervious areas were assigned a rational coefficient of 0.35, representative of lawns on average slope and low permeability soil (Chin 2006). An area-weighted rational coefficient was utilized to determine peak inflow rates.

Weir equations related outflow to depth of flow above each weir crest (Grant and Dawson 2001):

$$Q = 571.4 \times H^{2.5}, 45^{\circ} \text{ v-notch weir} \quad (3)$$

$$Q = 796.7 \times H^{2.5}, 60^{\circ} \text{ v-notch weir} \quad (4)$$

where Q is flow rate (L/s) and H is head (m) above the weir crest. Outflow rates were calculated on a 2-minute interval, and the area under the hydrograph integrated over time to calculate outflow volume on a storm-by-storm basis. Cumulative inflow and outflow volumes were the sum of individual storm volumes. The peak outflow rate for each storm event was the maximum instantaneous 2-minute value.

Hydrograph separation was used at HA to separate drainage from overflow following methods proposed in Brown and Hunt (2011a). Modeling in USEPA's Storm Water Management Model (SWMM) v5.1.007 was performed to separate drainage from overflow at UC (USEPA 2015). A rating curve was developed in SWMM to predict drainage based on measured internal water level data (Winston 2016). Assumptions were made that (1) all water stored in the bioretention media and aggregate layers was hydraulically connected, and (2) the hydraulic conductivity was sufficient enough that the internal water level measured in observation wells reflected a true water surface elevation. Measured internal water levels then represented the driving head for drainage.

To develop the rating curve, the bioretention cell was modeled as a storage unit in SWMM with a conduit controlling discharge (i.e., pressurized pipe flow). The outlet was modeled as a 10-m length of PVC pipe (Manning's roughness of 0.011) to account for friction losses from the underdrain and fittings. A resulting internal water level-discharge relationship was used to generate a drainage hydrograph for each monitored storm event.

To determine the combined volume of exfiltration and evaporation, internal water level measurements within the bioretention media were utilized to calculate the drawdown rate. Following each storm, the water level and date/time of the end of drainage (i.e., when the water level reached the invert of the underdrain) were recorded. Immediately preceding the commencement of the following rain event, the water level and date/time were also recorded. A total drawdown time and depth could then be calculated; the drawdown rate (mm/hr) is defined as the quotient of these values. The total volume of exfiltration and ET was calculated using:

$$V_{EE} = \frac{\sum_{i=1}^{n}(Q_{DD,i} \times t_{DD,i} \times \phi) \times f_{drain} \times A_{IS}}{1000} \quad (5)$$

where V_{EE} is the total volume exfiltrated and evapotranspired over the monitoring period (m^3), n is the total number of inter-event periods, Q_{DD} is the drawdown rate (mm/hr), t_{DD} is the inter-event period duration (hr), ϕ is the porosity of the aggregate and/or bioretention media [measured during determination of soil-water characteristic curves, Winston (2016)], f_{drain} is the ratio of the total monitoring period duration to the total dry period duration, and A_{IS} is the area of the infiltrative surface (m^2). The f_{drain} parameter accounted for drawdown during periods of drainage.

3.3 Analysis of Soil Hydraulic Conductivity

Construction was temporarily suspended at UC as excavation reached the final subgrade elevation to undertake soil testing (Figure 4). Prior to construction at HA, test pits were excavated at the locations of proposed bioretention cells for the same purpose. Two single-ring, constant head K_{sat} tests were completed in the subsoils beneath each of the HA cells (Reynolds et al. 2002); three such tests were undertaken at UC. A hoe was used to remove loose soil and create a level test surface of uncompacted subsoil. A Mariotte bottle kept a constant head of 15

cm, and mathematical corrections were used to account for lateral water flow (Reynolds et al. 2002). The tests estimated vertical K_{sat} through the bottom of the bioretention cell. These measurements were compared against post-construction drawdown rates to determine factors responsible for volume reduction and whether soil testing prior to or during construction was a reasonable indicator of post-construction drawdown rates.

Figure 4. Single ring infiltrometer with Mariotte bottle used for pre-construction infiltration testing (left) and monitoring well used for post-construction drawdown rate measurement (right).

3.4 Determination of the Bioretention Abstraction Volume

The Bioretention Abstraction Volume (BAV) was defined by Davis, Traver et al. (2012) as the volume of water captured by the bioretention cell and either exfiltrated or evapotranspired. Soil storage availability is affected by soil moisture conditions: saturation (SAT, all pores filled), field capacity (FC, water drained under gravity), and wilting point (WP, the water content where plants can no longer extract water for ET). As defined in Davis, Traver et al. (2012), theoretical BAV is calculated using:

$$\text{Low BAV} = \text{RZMS} \times (\text{SAT-WP}) \quad (6)$$

$$\text{Average BAV} = \text{RZMS} \times (\text{SAT-WP}) + \text{LMS} \times (\text{SAT-FC}) \quad (7)$$

$$\text{High BAV} = \text{Surface Storage Volume} + \text{RZMS} \times (\text{SAT-WP}) + \text{LMS} \times (\text{SAT-FC}) \quad (8)$$

where RZMS is the volume of the media (m^3) in the root zone and LMS is the volume of media below the root zone but above the IWS zone (m^3). In this study, the root zone was assumed to be 30 cm since plants were juvenile during the study.

4 Results and Discussion

4.1 Rainfall

Over the monitoring period at UC (May to November 2014), fifty storm events were observed. The monitoring period at HA was from October 2013 through November 2014, during which 90 separate storms were reliably monitored. Data collected during the winter (December 2013 through March 2014) at HA were not included in this analysis due to sub-freezing temperatures.

Total rainfall depths during the monitoring periods at UC and HA were 742 and 1175 mm, respectively. Over the 30-yr period from 1981-2010, Cleveland Hopkins International Airport (the nearest long-term rainfall record) received an annual average of 994 mm of precipitation (NOAA 2015); precipitation depth during the monitoring periods was greater than the long-term average at both sites. Median and mean rainfall depths were 7-8 mm and 13-14 mm, respectively (Table 2). Maximum event depth was 89 mm at UC and 71 mm at HA. Median and mean ADP ranged from 2 to 4 days.

At UC and HA, respectively, the 79th and 80th percentile observed events corresponded to the 19-mm water quality design event for Ohio. Since they were oversized, the UC, HA South, and HA North treated without overflow the 86th, 96th, and 96th percentile observed rainfall depths, respectively. Therefore, the hydrologic performance of these bioretention cells was expected to exceed that of the typical bioretention design in northeast Ohio.

Table 2. Summary statistics for rainfall events at UC and HA.

Monitoring Site	Statistic	Depth (mm)	Average intensity (mm/hr)	Peak 5-minute rainfall intensity (mm/hr)	Antecedent Dry Period (days)
UC	Minimum	2.5	0.3	3.0	0.3
	Median	8.1	1.4	16.8	2.2
	Mean	14.4	2.3	29.2	3.5
	90th percentile	39.3	4.9	74.7	7.9
	Maximum	89.2	12.9	152.4	20.0
HA	Minimum	2.5	0.3	3.0	0.3
	Median	7.1	1.2	9.1	2.6
	Mean	12.7	2.8	22.6	4.0
	90th percentile	31.0	5.6	56.1	8.6
	Maximum	70.9	49.5	103.6	19.7

4.2 Drawdown Rate

The underlying soil properties are important to bioretention cell hydrology (Brown and Hunt 2010). If compaction of underlying soils is prevented during construction, pre-construction field-measured saturated hydraulic conductivity (K_{sat}) tests can help predict long-term bioretention hydrology (Pitt et al. 2008; Tyner et al. 2009; Wardynski et al. 2012).

Underlying soil saturated hydraulic conductivities were measured during construction and were representative of the mapped HSG D soils (Table 3; USDA-NRCS 2007): 0.5 and 0.5 mm/hr at HA North, 0.5 and 2 mm/hr at HA South, and 0.5, 0.5, and 0.75 mm/hr at UC. While these vertical K_{sat} measurements do not quantify all of the processes that determine the post-construction drawdown rate (for reasons discussed below), they are likely the most useful predictor of drawdown rate.

Following construction, internal water level measurements were used to calculate drawdown rates for each bioretention cell. Drawdown rates for the bioretention cells were non-linear, but average values shown in Table 3 typically are used in hydrologic modeling (Smolek et al. 2015).

Post-construction drawdown rates were up to 6- to 8-fold (at UC) and 3- to 4-fold (at HA) *higher* than the K_{sat} measured during construction (Table 3).

Table 3. Comparison of saturated hydraulic conductivity (K_{sat}) measured during construction to post-construction drawdown rate.

Site	K_{sat} measured during construction (mm/hr)	Drawdown rate (average ± standard deviation, mm/hr)
UC	0.5, 0.5, 0.75	4.3 ± 4.3
HA North	0.5, 0.5	1.7 ± 1.2
HA South	0.5, 2.0	2.0 ± 3.5

There are a number of potential reasons for this disparity between the two measurements. During construction, the teeth of the excavator bucket were drawn across the subsoil to break up compaction before backfilling with aggregate and media, as recommended by Brown and Hunt (2010). The small number of pre-construction K_{sat} tests (2-3) may not wholly characterize the potential for exfiltration or provide a representative average K_{sat}, as flow favors (potentially unmeasured) higher permeability areas. Soil K_{sat} may vary over two orders of magnitude within a given SCM (Asleson et al. 2009; Wardynski and Hunt 2012; Olson et al. 2013).

Because the bioretention cells were either irregularly shaped (HA) or long and thin (UC), the proportion of side-walls was relatively high, encouraging lateral exfiltration, which was not captured in vertical K_{sat} measurements during construction. When the IWS zones were completely full, the side-wall surface area represented 27%, 20%, and 22% of the total (i.e., side-wall plus subgrade) exfiltrative surface area at UC, HA South, and HA North, respectively. Lateral exfiltration occurs at a rate proportional to the lateral K_{sat}. The ratio of vertical to lateral K_{sat} varies spatially and as a function of soil horizon and texture (Bathke and Cassel 1991), but lateral K_{sat} is generally higher than vertical K_{sat} in clay soils, often by factors of 10 to 25 (Bathke and Cassel 1991). Modeling of exfiltration from urban SCMs has shown lateral exfiltration is

often the dominant pathway for volume reduction (Browne et al. 2008; Lee et al. 2015). Additionally, ET was responsible for a modest portion of the drawdown, especially during summer months. For these reasons, drawdown post-construction was higher than vertical K_{sat} measurements obtained during construction; a similar result was not found for permeable pavements in this region of Ohio (Winston, Dorsey et al., submitted). This supports the installation of many distributed bioretention cells within a watershed, which will provide better hydrologic mitigation than a single large system due to greater lateral exfiltration.

A subset of the internal water level data for UC is shown in Figure 5. Water levels above the IWS zone (0.6-m thick) corresponded to periods of drainage. The near-vertical water level recession curve between 0.6 and 0.38 m is likely due to very high lateral K_{sat} in this soil horizon (Bathke and Cassel 1991) and/or to greater driving head for vertical exfiltration. A slope break in the drawdown curve was present at 0.38 m; below this point exfiltration occurred at a lower rate approximated by an exponential decay, similar to Schlea et al. (2014). Drawdown below the 0.03-m internal water level represented the transition from head driven exfiltration to capillary flow.

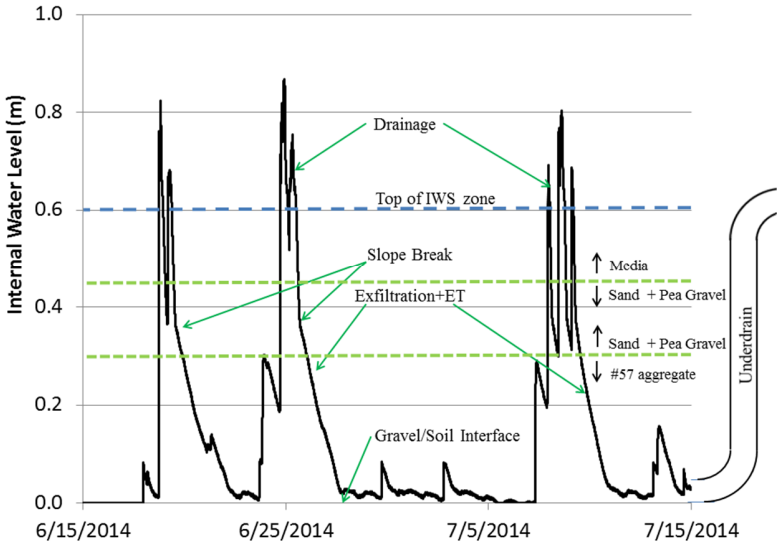

Figure 5. Excerpt of UC internal water levels during June-July 2014.

The HA South and North cells had IWS zone thicknesses of 0.38 and 0.45 m (Figure 6). Drawdown rates again were non-linear and modeled using an exponential decay; Lee et al. (2015) suggested nonlinear drawdown curves were representative of SCMs dominated by lateral exfiltration. This is primarily due to the changes in wetted side-wall surface area and decreased driving head with drawdown. Drawdown rates were, on average, about 25% higher for HA South than HA North (Figure 6), demonstrating the spatial variability of soils (the cells were located 20 m apart) and resulting in the South cell's better volume reduction (discussed later). Both HA cells tended to shift from head driven exfiltration to capillary flow at a 0.1-m internal water level.

Drawdown rates would be expected to vary diurnally if ET was a substantial contributing factor to volume reduction (Vaughn et al. 2007). In Figures 5 and 6, the drawdown rate is not more rapid during the day (when ET would be at its highest) than it is overnight (when ET is reduced). Therefore, the sum of transpiration provided by the juvenile plants and evaporation did not substantially impact overall bioretention hydrology. The original intent of the HA study

was to observe bioretention performance under two different plant palettes: shrubs and trees versus forbs and perennial grasses. However, differences in exfiltration rates discussed above confounded this effort.

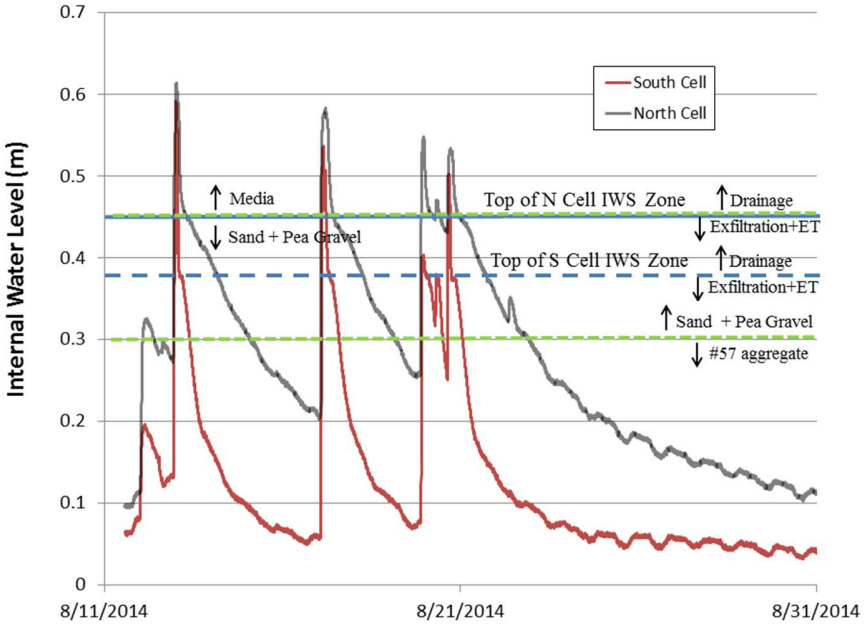

Figure 6. HA North and South bioretention cell internal water level profiles during August 2014.

4.3 Hydrograph Separation using SWMM

All outflow from each bioretention cell passed over a single weir; therefore, hydrograph analysis was employed to separate drainage from overflow. A depth-discharge rating curve was used to generate storm event drainage hydrographs at UC based on a calibrated USEPA SWMM V5.1 model (Figure 7). The difference between the measured outflow hydrograph and the modeled drainage hydrograph was the amount of overflow that occurred. This provided a more representative estimate of overflow than visual hydrograph separation, since drain flow under pressurized conditions should be dependent on internal water level. This type of hydrologic

modeling can help inform field-collected data and improve the understanding of unit processes within an SCM (Smolek et al. 2015).

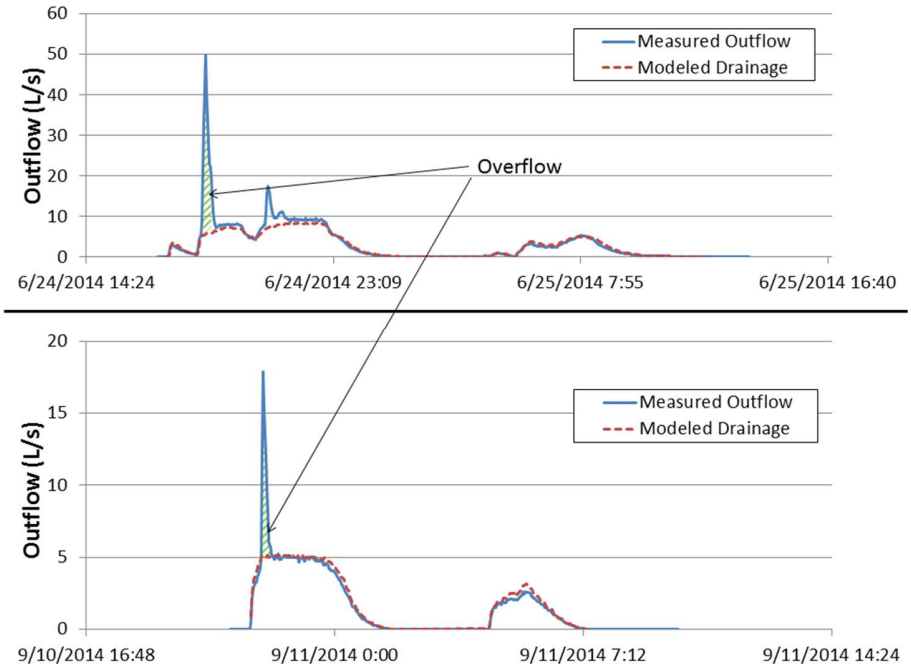

Figure 7. Measured outflow and modeled drainage hydrographs for UC. Modeling was completed in US EPA SWMM model V5.1.

4.4 Volume Reduction

Over the monitoring periods, the three monitored bioretention cells reduced runoff volume (i.e., the sum of exfiltration and ET) by 59% (UC), 42% (HA South), and 36% (HA North, Table 4). The greatest volume reduction was achieved by the cell with the largest drawdown rate and thickest IWS zone. While few studies of bioretention cells constructed in low conductivity soils have been published, Sansalone and Teng (2004) found 55-70% exfiltration from an infiltration-based SCM (termed a partial exfiltration reactor) located in low permeability glacial till soils in Cincinnati, OH. Two bioretention cells built in compacted, low permeability soils and incorporating 0.6-m IWS zones reduced runoff volume by 20% and 30% when designed to capture the 12.5 and 25-mm events, respectively (Luell 2011). Cells employing IWS and built in

conductive soils provided more volume reduction (e.g., 75-87% in sandy clay loam and 96-100% in sand; Brown and Hunt 2011b).

Table 4. Summary statistics for volume and percentage of inflow, drainage, overflow, and exfiltration/ET over the monitoring periods.

Cell Name	Total Inflow (mm)	Drainage (mm)	Overflow (mm)	Exfiltration + ET (mm)	Drainage (%)	Overflow (%)	Exfiltration/ET (%)
UC	570	189	43	338	33.2	7.6	59.2
HA South	511	261	35	215	51.1	6.8	42.1
HA North	525	300	36	189	57.1	6.9	36.0

Drainage represented 33-57% of the overall water balance, depending on the bioretention cell. Generally, drainage should have lower pollutant concentrations when compared to those of untreated runoff (provided proper media is selected, Hunt et al. 2012; Iqbal et al. 2015; Mullane et al. 2015). Debusk et al. (2011) suggested drainage from bioretention cells was released at rates similar to post-storm event shallow interflow in rural reference streams, mimicking pre-development hydrology. Since drainage is controlled outflow, it should not cause erosion to the same extent as overflow or uncontrolled runoff.

Overflow represented about 7% of the water balance at HA. These bioretention cells were sized to capture the 44.7 and 45.2-mm events, more than two-fold larger than the water quality event in Ohio. . Overflow was 7.6% of the water balance at UC. In this study, overflow represented less of the water balance than in past studies on bioretention cells, which ranged from 11 to 23% (Li et al. 2009; Brown and Hunt 2012). A bioretention cell sized for the 19-mm water quality event in Ohio would experience more overflow under similar conditions.

DRAINMOD modeling results suggested ET represented between 4.5-5.5% of the overall water balance for each of the bioretention cells (Winston, Smolek et al. submitted), similar to the 3% ET observed for cells in North Carolina (Brown and Hunt 2012). Evapotranspiration was

19% of inflow for a lined bioretention cell in Louisburg, NC (Li et al. 2009). Modeling of bioretention with RECARGA suggested ET was about 1% of the overall water balance (Hoskins and Peterein 2013). Based on lysimeter data, Wadzuk et al. (2014) indicated bioretention employing IWS and sized to treat 5% of its impervious catchment would evapotranspire 4% of the overall water balance.

Low Impact Development strategies focus on abstraction of small storm events to reduce stormwater volume (Davis 2008). In this study, between 31-68% of observed rainfall events were completely captured (i.e., no drainage or overflow) by the bioretention cells (Table 5). For comparison, no outflow occurred during 27-63% of events at four bioretention cells in NC and MD (Li et al. 2009). Thirty-three percent of events were completely captured in a lined (to prevent exfiltration) bioretention cell in Australia (Hatt et al. 2009). Events up to 14-mm depth were completely captured, albeit different ADPs were required (9 days at HA and 1.5 days at UC). Higher exfiltration rates at UC allowed faster dewatering of the IWS zone and consequently greater storage when ADP was short.

Table 5. Summary of completely captured storm events (i.e., no outflow).

Cell name	Events completely captured (#)	Range of rainfall depths of completely captured events (mm)	Percentage of events completely captured
UC	34/50	2.5-14	68
HA South	44/90	2.5-13	49
HA North	28/90	2.5-13	31

Average BAV was determined by regressing outflow volume against inflow volume for each bioretention cell and using segmented linear regression to determine the slope and intercept of the bioretention response following abstraction (Table 6). The field-derived BAV for the three cells differed substantially, from 3.4±1.3 m^3 (BAV±95% confidence interval [CI]) for HA North,

4.5±1.8 for HA South, and 28.2±15.9 for UC. The wider CI at UC is indicative of the lower number of outflow-producing events (Table 5).

The HA cells had lower drawdown rates and smaller IWS zone thicknesses and were therefore able to abstract much less volume than UC. Field-derived BAVs for the HA cells were similar to the theoretical low BAV and well below the surface storage volume, suggesting outflow began well before the surface storage zone was full. The IWS zones at the HA cells often were near-full at the commencement of rainfall, limiting their abstraction capacity. At UC, average BAV (21.1 m^3) was lower than field-derived BAV (28.2 m^3), suggesting this method may need to be modified to account for IWS zone storage (given typical ADPs). Once the bioretention cells entered the outflow production phase, the slope of the outflow trendline at UC was lower (0.76) than at HA (0.87-0.88), suggesting greater volume reduction at UC during large events, perhaps related to intra-event drawdown.

A few modifications to the BAV calculation presented by Davis, Traver et al. (2012) are suggested for cells incorporating IWS. The IWS zone provides additional storage below the underdrain invert:

$$\text{Average BAV} = \text{RZMS} \times (\text{SAT-WP}) + \text{LMS} \times (\text{SAT-FC}) + Q_{DD,Avg} \times \boldsymbol{\phi} \times ADP_{Avg} \times SA \quad (9)$$

where $Q_{DD,Avg}$ is the average drawdown rate (mm/hr), $\boldsymbol{\phi}$ is the porosity of the aggregate or media (unitless), ADP_{Avg} is the average ADP (hours) calculated over a long-term period of record, and SA is the surface area of the cell. For cells with considerable exfiltration rates, the IWS zone provides a substantial amount of additional storage. Furthermore, the results from the HA cells suggest the surface storage volume should not be included in the calculation of the high BAV for cells with an underdrain and constructed over poorly drained soils. When the bowl is full, the

media will be saturated or nearly saturated, meaning that at the cessation of rainfall, most of the water stored in the bowl will drain through the underdrain.

Table 6. Statistics for bioretention abstraction volume for the three bioretention facilities.

Characteristics	UC	HA South	HA North
Field-derived			
Ave. BAV (m^3)	28.2	4.5	3.4
95% CI on BAV (m^3)	±15.9	±1.8	±1.3
Slope of best-fit line	0.76	0.88	0.87
Theoretical BAV			
Low BAV (m^3)	16.6	5.5	5.9
Ave. BAV (m^3)	21.1	7.8	8.4
High BAV (m^3)	81.1	42.8	56.4

There are two phases of bioretention hydrology: (1) abstraction and (2) outflow production. During abstraction, practically all events below a threshold rainfall depth, the D_T, produce zero outflow (Hood et al. 2007). Using segmented linear regression, the D_T was 13.8, 7.4, and 5.5 mm for UC, HA South, and HA North, respectively; bootstrapping was performed to determine the 95% confidence interval around the D_T (Figure 8). While UC was built to capture a smaller rainfall depth (Table 1), the thicker IWS zone and 2-2.5 times greater exfiltration rate resulted in greater abstraction. Once outflow began, the steeper slope of the outflow volume best-fit line for UC was indicative of the larger catchment area, higher percentage imperviousness, and directly connected impervious area (Figure 8). Discharge thresholds in this study were similar to (HA cells) or higher (UC) than those reported for LID developments in Connecticut (Hood et al. (2007) and North Carolina (Page et al. 2015a), which were 3-6 mm.

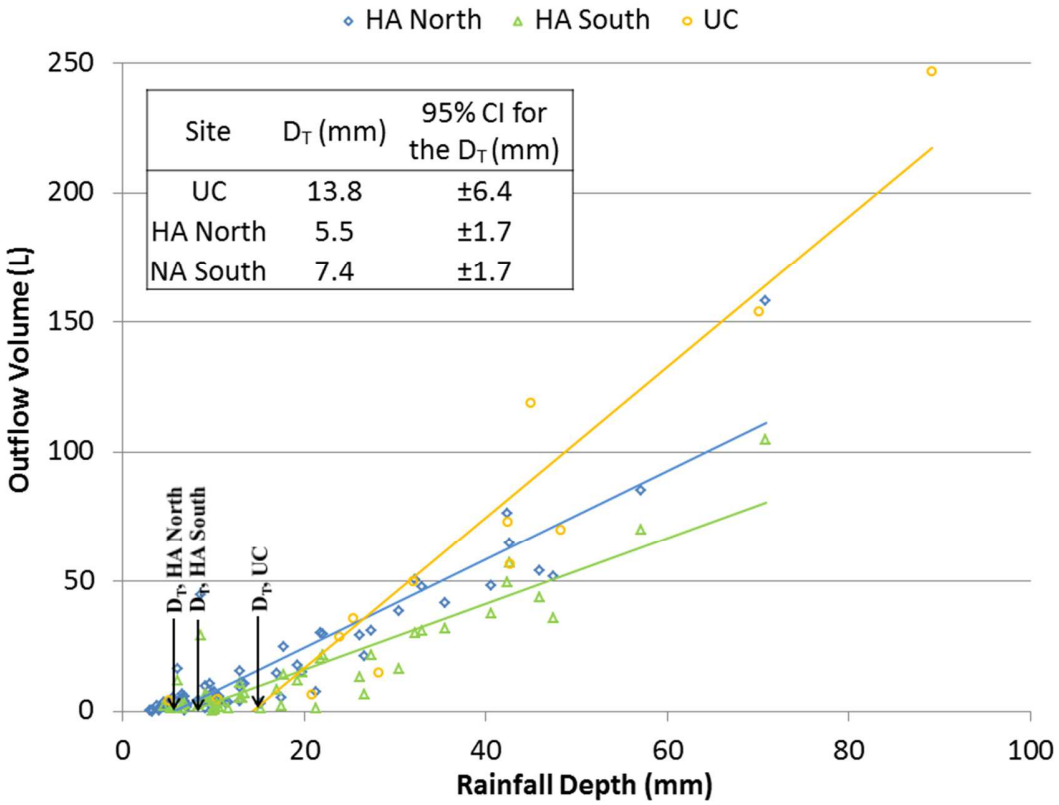

Figure 8. Determination of the discharge threshold for the bioretention facilities. Events with zero outflow were omitted for clarity.

Figure 9 depicts the volume discharge ratio (VDR), defined as the event-by-event ratio of outflow to inflow volume. Data were plotted as ranked probability distributions, as suggested in Piechota et al. (2001). Zero-outflow events were plotted at 0.001 VDR for inclusion on the log-scale plot.

Twenty-six percent of events at UC had substantial outflow (VDR>0.1), 6% of events produced minor outflow (0<VDR<0.1), and 68% were completely captured. The HA South and North cells (both with lower drawdown rate than UC) produced substantial outflow during 44% and 54% of events and minor outflow during 5% and 10% of events, respectively, highlighting the importance of drawdown rate to volume reduction (Table 3). Volume reduction occurred in

all monitored storms, with the bioretention cells abstracting at minimum 14% of the inflow volume.

Davis (2008) suggested a VDR less than or equal to 0.33 as a target for LID efficacy. Two bioretention cells in Maryland met this target for 54% and 61% of observed events (Davis 2008). The HA North, HA South, and UC cells had VDR<0.33 for 51%, 67%, and 82% of events. The two cells in Maryland incorporated impermeable liners for research purposes, eliminating exfiltration, and explaining why UC, with a moderate drawdown rate of 4.3 mm/hr, exhibited better performance. Undersized bioretention cells in North Carolina met this criterion for 44% of events (Brown and Hunt 2011a).

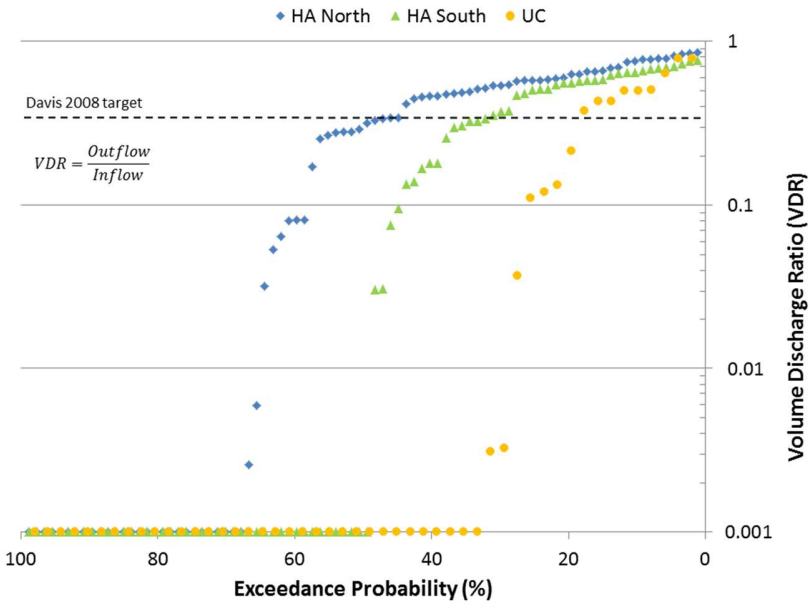

Figure 9. Exceedance probability for volume discharge ratio.

4.5 Peak Flow Mitigation and Flow Duration

Peak flow mitigation was greatest for the smallest rainfall intensities, as the bowl completely stored the event, eliminating overflow and limiting outflow rates to the drainage capacity of the underdrain (Table 7). Similar results have been found in other bioretention studies (Davis 2008;

Hatt et al. 2009; Brown and Hunt 2012). Generally, as rainfall intensity increased, peak flow mitigation decreased, especially for storms with overflow. For the three bioretention cells, peak flow mitigation was a minimum of 29% (except for one storm at HA North with no peak flow mitigation).

Oversized bioretention systems decrease the number of overflow producing events by providing greater bowl storage volume; for instance, only 10, 12, and 12 events at UC, HA South, and HA North, respectively, exceeded the design storage capacity of the bowl. Had the cells been sized to capture only the runoff volume from the 19-mm water quality event, the number of events with overflow would have increased to 11, 19, and 19. Oversizing a bioretention cell with respect to its catchment area caused the most marked changes in long-term fraction of overflow during bioretention hydrologic simulations in DRAINMOD (Winston, Smolek et al. submitted). Deeper bowl depths are one method to accomplish this.

Table 7. Statistics for peak flow mitigation at the UC and HA bioretention cells.

Site Name	Location	Median Peak Flow Rate (L/s)	75th Percentile Peak Flow Rate (L/s)	90th Percentile Peak Flow Rate (L/s)	Maximum Peak Flow Rate (L/s)	Median Peak Flow Reduction (%)	Range of Peak Flow Reduction (%)
UC	Inflow	10.5	25.2	45.2	105.0	100	50-100
	Outflow	0.0	0.2	8.0	49.9		
HA South	Inflow	3.9	8.7	23.2	32.7	98.9	29-100
	Outflow	0.1	0.6	1.8	23.3		
HA North	Inflow	6.1	13.7	36.8	51.9	96.6	0-100
	Outflow	0.2	0.7	2.7	36.6		

Stormwater controls are often designed to mitigate flood risk for storms greater than the 1 year event. Design rainfall event intensities were obtained for Cleveland Hopkins International airport, the nearest reliable source of long term data (located approximately 39 km from UC and 60 km from HA) (NOAA 2015). Because the times of concentration from the catchments of

interest were small (i.e., less than 5 minutes), a 5-minute rainfall duration was used for this analysis. During the monitoring period, five events occurred at HA with peak rainfall intensities exceeding the 1-yr, 5-minute rainfall intensity (99 mm/hr); four such events occurred at UC – of those, one event exceeded the 5-yr, 5-minute (141 mm/hr) rainfall intensity. While all four such events at UC exceeded the bowl storage capacity of 29.5 mm, peak outflow rates were still reduced by 53-88%. In all cases, the peak rainfall intensity occurred within the first few hours of the hyetograph, before the bowl filled. Outflow rates were then restricted by the K_{sat} of the media and the capacity of the underdrain. At HA, only 3 of the 5 intense events produced overflow. Peak flow reductions for these three events ranged from 24-96%. Even during events with overflow, substantial peak flow mitigation was provided by the UC (worst case 53%) and HA (worst case 24%) bioretention cells. These results suggest that center-weighted design hyetographs (wherein the majority of the rainfall arrives over a 3 hour period) may not represent observed rainfall patterns, resulting in conservative SCM designs for peak flow mitigation.

Flow duration curves were used to summarize the hydraulic response of bioretention cells by amalgamating outflow rates measured on a 2-minute interval across all observed storm events into a single distribution (Figure 10; Davis, Stagge et al. 2012). The monitoring period duration was 209 days at UC and 304 days at HA. Outflow from the UC bioretention cell occurred for 82 hours, or 1.6% of the monitoring period. For the HA South and North cells, outflow duration was 464 and 1099 hours, respectively, representing 6.4 and 15.1% of the monitoring periods. The total duration of rainfall during the monitoring periods was 452 and 821 hours at UC and HA, respectively. For bioretention facilities providing considerable exfiltration (UC), the duration of outflow will be substantially reduced, while lower drawdown rates (e.g., HA North) may result in periods of drainage extending beyond rainfall duration. Similar elongated outflow

durations were observed by Davis (2008) for two lined bioretention cells and for retention basins in Roesner et al. (2001) and Tillinghast et al. (2011). Stormwater control measures promoting volume reduction have been shown to reduce duration of outflow from urban impervious surfaces by up to 50% (Davis, Stagge et al. 2012).

The duration of outflow from a bioretention cell is related primarily to the IWS zone thickness, exfiltration rate, and bowl storage volume. Regardless of underlying soil type, the reduced outflow volume from bioretention facilities will reduce bed load transport and/or potential bank erosion (Pomeroy et al. 2008).

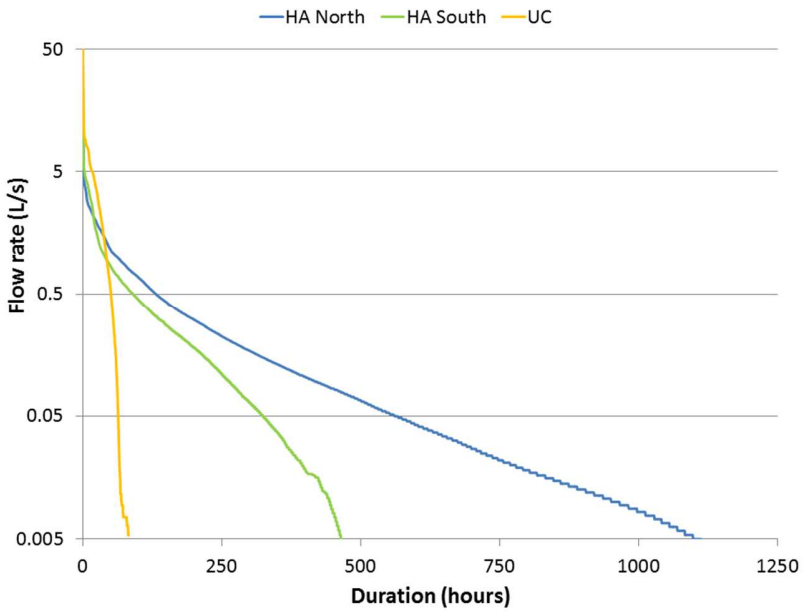

Figure 10. Flow duration curves for outflow from the bioretention cells.

5 Summary and Conclusions

Three bioretention cells constructed over low conductivity soils were evaluated for hydrologic performance in northeast Ohio. The water balance was quantified at each site, and volume reduction, peak flow mitigation, and flow duration were related to design characteristics. The following conclusions may be drawn from this study:

1) Vertical K_{sat} is an intensive property of the soil underlying the bioretention cell, whereas drawdown rate in the IWS zone is dependent on other factors, including driving head, IWS zone depth, and lateral soil K_{sat}. Measured post-construction drawdown rates for all three bioretention cells exceeded the measured vertical K_{sat} of the soils underlying the bioretention cells. This was likely due to lateral exfiltration through the side walls of the bioretention cells, increased head (compared to the infiltration testing) in the IWS zones, and relatively minor amounts of ET. These results support the installation of a greater number of smaller, distributed bioretention systems, as opposed to one large SCM, to drive additional exfiltration by augmenting the side-wall surface area. The incorporation of an IWS zone is also critical to lateral exfiltration.

2) Runoff reduction for the UC, HA South, and HA North cells was 59%, 42%, and 36%, primarily related to the drawdown rates of the underlying soils. Discharge thresholds were 13.8, 7.4, and 5.5 mm, respectively, showing that bioretention cells eliminate outflow from small events even when situated over low permeability soils. Substantial volume reduction can occur when bioretention cells are situated over poorly drained soils, especially with the inclusion of an IWS zone that exfiltrates stormwater during inter-event periods. Underlying soil conductivity should not be a restricting factor for bioretention cell installation.

3) During events exceeding the 1-yr, 5-minute rainfall intensity, the UC and HA cells provided 53-88% and 24-96% peak flow mitigation, respectively. The peak rainfall rate often occurred well before the centroid of the rainfall volume, meaning there was adequate bowl storage to mitigate peak inflow rates without producing overflow. These results combined with those for volume reduction support the installation of oversized bioretention cells to control outflow rates from smaller design rainfall events.

4) The UC, HA South, and HA North cells produced outflow during 18%, 56%, and 134% of the total rainfall duration; flow duration was directly related to the underlying soil conductivity, IWS zone thickness, and bowl storage volume. The duration of outflow from SCMs will be critical as the profession moves from single-storm peak flow based designs to pre- and post-development hydrograph matching.

6 Acknowledgements and Disclaimer

The authors thank the National Oceanic and Atmospheric Administration (NOAA) for their financial support of this work. We appreciate the efforts of Kevin Grieser of Biohabitats, Inc., and the staffs of Chagrin River Watershed Partners and Old Woman Creek National Estuarine Research Reserve, who assisted in various phases of the project. The Holden Arboretum and Ursuline College are acknowledged for hosting the research sites.

This work was supported by the University of New Hampshire under Cooperative Agreement No. NA09NOS4190153 (CFDA No. 11.419) from the National Oceanic and Atmospheric Administration. Any opinions, findings, and conclusions or recommendations expressed in this publication are those of the author(s) and do not necessarily reflect the views of the University of New Hampshire or the National Oceanic and Atmospheric Administration.

7 References

American Society for Testing and Materials (ASTM), 2007. Standard test method for particle-size analysis of soils. ASTM D422-63.

American Society for Testing and Materials (ASTM), 2012. Standard classification for sizes of aggregate for road and bridge construction. ASTM D448-12.

American Society for Testing and Materials (ASTM), 2014. Standard test methods for moisture, ash, and organic matter of peat and other organic soils. ASTM D2974-14.

Asleson, B.C., Nestingen, R.S., Gulliver, J.S., Hozalski, R.M., Nieber, J.L., 2009. Assessment of rain gardens by visual inspection and controlled testing. J. Am. Water Resour. Assoc. 45, 1019–1031.

Autixier, L., Mailhot, A., Bolduc, S., Madoux-Humery, A.S., Galarneau, M., Prévost, M., Dorner, S. 2014. Evaluating rain gardens as a method to reduce the impact of sewer overflows in sources of drinking water. Sci. Total Environ. 499, 238-247.

Bathke, G.R., Cassel, D.K., 1991. Anisotropic variation of profile characteristics and saturated hydraulic conductivity in an Ultisol landscape. Soil Sci. Soc. Am. J. 55(2), 333-339.

Blecken, G.T., Zinger, Y., Deletić, A., Fletcher, T.D., Viklander, M., 2009. Impact of a submerged zone and a carbon source on heavy metal removal in stormwater biofilters. Ecol. Eng. 35(5), 769-778.

Bledsoe, B., Watson, C., 2001. Effects of urbanization on channel instability. J. Am. Water Resour. Assoc. 37(2), 255–270.

Booth, D.B., 1990. Stream-channel incision following drainage-basin urbanization. J. Am. Water Resour. Assoc. 26(3), 407-417.

Booth, D., Hartley, D., Jackson, R., 2002. Forest cover, impervious surface area, and the mitigation of storm-water impacts. J. Am. Water Resour. Assoc. 38(3), 835–845.

Bratieres, K., Fletcher, T.D., Deletic, A., Zinger, Y., 2008. Nutrient and sediment removal by stormwater biofilters: A large-scale design optimisation study. Water Res. 42(14), 3930-3940.

Brown, R.A., Hunt, W.F., 2010. Impacts of construction activity on bioretention performance. J. Hydrol. Eng. 15(6), 386-394.

Brown, R.A., Hunt, W.F., 2011a. Impacts of media depth on effluent water quality and hydrologic performance of under-sized bioretention cells. J. Irrig. Drain. Eng. 137(3), 132-143.

Brown, R.A., Hunt, W.F., 2011b. Underdrain configuration to enhance bioretention exfiltration to reduce pollutant loads. J. Environ. Eng. 137(11), 1082-1091.

Brown, R.A., Hunt, W.F., 2012. Improving bioretention/biofiltration performance with restorative maintenance. Water Sci. Technol. 65(2), 361-367.

Browne, D., Deletic, A., Mudd, G.M., Fletcher, T.D., 2008. A new saturated/unsaturated model for stormwater infiltration systems. Hydrol. Processes 22(25), 4838–4849.

Burns, M.J., Fletcher, T.D., Walsh, C.J., Ladson, A.R., Hatt, B.E., 2012. Hydrologic shortcomings of conventional urban stormwater management and opportunities for reform. Landscape Urban Plann. 105(3), 230-240.

Chen, Y., Day, S.D., Wick, A.F., McGuire, K.J. 2014. Influence of urban land development and subsequent soil rehabilitation on soil aggregates, carbon, and hydraulic conductivity. Sci. Total Environ. 494, 329-336.

Chin, D.A., 2006. Water resources engineering. 2nd edition. Pearson Prentice Hall, Upper Saddle River, NJ.

City of Omaha, 2014. Omaha regional stormwater design manual. Chapter 8: Stormwater best management practices. City of Omaha environmental quality control division. Available: http://www.omahastormwater.org/download/chapter-8-stormwater-best-management-practices/

Cizek, A.R., Hunt, W.F., 2013. Defining predevelopment hydrology to mimic predevelopment water quality in stormwater control measures (SCMs). Ecol. Eng. 57, 40-45.

Davis, A.P., 2008. Field performance of bioretention: hydrology impacts. J. Hydrol. Eng. 13(2), 90-95.

Davis, A.P., Hunt, W.F., Traver, R.G., Clar, M., 2009. Bioretention technology: Overview of current practice and future needs. J. Environ. Eng. 135(3), 109-117.

Davis, A.P., Stagge, J.H., Jamil, E., Kim, H., 2012. Hydraulic performance of grass swales for managing highway runoff. Water Res. 46(20), 6775-6786.

Davis, A.P., Traver, R.G., Hunt, W.F., Lee, R., Brown, R.A., Olszewski, J.M., 2012. Hydrologic performance of bioretention storm-water control measures. J. Hydrol. Eng. 17(5), 604-614.

DeBusk, K.M., Hunt, W.F., Line, D.E., 2011. Bioretention outflow: Does it mimic nonurban watershed shallow interflow? J. Hydrol. Eng. 16(3), 274-279.

Dietz, M.E., Clausen, J.C., 2005. A field evaluation of rain garden flow and pollutant treatment. Water Air Soil Poll. 167(1-4), 123-138.

Dietz, M.E., Clausen, J.C., 2006. Saturation to improve pollutant retention in a rain garden. Environ. Sci. Technol. 40(4), 1335-1340.

Emerson, C., Traver, R., 2008. Multiyear and seasonal variation of infiltration from storm-water best management practices. J. Irrig. Drain. Eng. 134(5), 598-605.

Fangmeier, D.D., Elliot, W.J., Workman, S.R., Huffman, R.L., Schwab, G.O., 2006. Soil and water conservation engineering. 5th edition. Thomson Delmar learning, Clifton Park, NY.

Grant, D.M., Dawson, B.D., 2001. Isco open channel flow measurement handbook. 5th edition. Isco, Inc., Lincoln, NE.

Guo, J.C., Luu, T.M., 2015. Operation of Cap Orifice in a Rain Garden. J. Hydrol. Eng. 20(10), 1-6. 06015002

Hamel, P., Daly, E., Fletcher, T.D., 2015. Which baseflow metrics should be used in assessing flow regimes of urban streams? Hydrol. Processes. 29(20), 4367-4378.

Hammer, T.R., 1972. Stream channel enlargement due to urbanization. Regional Science Research Institute Discussion Paper Series, No. 55. Philadelphia, PA, 41 pp.

Hatt, B.E., Fletcher, T.D., Deletic, A., 2009. Hydrologic and pollutant removal performance of stormwater biofiltration systems at the field scale. J. Hydrol. 365(3), 310-321.

Heasom, W., Traver, R.G., Welker, A., 2006. Hydrologic modeling of a bioinfiltration best management practice. J. Am. Water Resour. Assoc. 42(5), 1329-1347.

Hood, M.J., Clausen, J.C., Warner, G.S., 2007. Comparison of stormwater lag times for low impact and traditional residential development. J. Am. Water Resour. Assoc. 43(4), 1036-1046.

Hoskins, J., Peterein, J., 2013. Case study of St. Louis, Missouri: Comparison of bioretention performance to the runoff component of a restored water balance. J. Environ. Eng. 139(4), 516-521.

Hunt, W.F., Jarrett, A.R., Smith, J.T., Sharkey, L.J., 2006. Evaluating bioretention hydrology and nutrient removal at three field sites in North Carolina. J. Irrig. Drain. Eng. 132(6), 600–608.

Hunt, W.F., Smith, J.T., Jadlocki, S.J., Hathaway, J.M., Eubanks, P.R., 2008. Pollutant removal and peak flow mitigation by a bioretention cell in urban Charlotte, NC. J. Environ. Eng. 134(5), 403-408.

Hunt, W.F., Davis, A.P., Traver, R.G., 2012. Meeting hydrologic and water quality goals through targeted bioretention design. J. Environ. Eng. 138(6), 698-707.

Iqbal, H., Garcia-Perez, M., Flury, M. 2015. Effect of biochar on leaching of organic carbon, nitrogen, and phosphorus from compost in bioretention systems. Sci. Total Environ. 521, 37-45.

Iowa Department of Natural Resources (IDNR), 2010. Iowa stormwater management manual. Chapter 2E: Infiltration practices. Available: http://www.iowadnr.gov/Environmental-Protection/Water-Quality/NPDES-Storm-Water/Storm-Water-Manual

Jenkins, J.K.G., Wadzuk, B.M., Welker, A.L., 2010. Fines accumulation and distribution in a storm-water rain garden nine years postconstruction. J. Irrig. Drain. Eng. 136(12), 862-869.

Jones, M.P., Hunt, W.F., 2009. Bioretention impact on runoff temperature in trout sensitive waters. J. Environ. Eng. 135(8), 577-585.

Klute, A., 1986. Water retention: Laboratory methods. Methods of soil analysis. Part 1:Physical and mineralogical methods, A. Klute, ed., Soil Science Society of America, Madison, Wis., 635–662.

Lee, J.G., Borst, M., Brown, R.A., Rossman, L., Simon, M.A., 2015. Modeling the hydrologic processes of a permeable pavement system. J. Hydrol. Eng. 20(5), 1-9.

Li, H., Sharkey, L.J., Hunt, W.F., Davis, A.P., 2009. Mitigation of impervious surface hydrology using bioretention in North Carolina and Maryland. J. Hydrol. Eng. 14(4), 407–415.

Lucas, W.C., Sample, D.J., 2015. Reducing combined sewer overflows by using outlet controls for Green Stormwater Infrastructure: Case study in Richmond, Virginia. Journal of Hydrology, 520, 473-488.

Lucke, T., Nichols, P.W. 2015. The pollution removal and stormwater reduction performance of street-side bioretention basins after ten years in operation. Sci. Total Environ. 536, 784-792.

Luell, S.K., 2011. Evaluating the impact of bioretention cell size and swale design in treating highway bridge deck runoff. M.S. thesis, Department of Biological and Agricultural Engineering, North Carolina State University.

Minnesota Pollution Control Agency (MPCA), 2015. Minnesota stormwater manual. Design criteria for bioretention. Available: http://stormwater.pca.state.mn.us/index.php/Design_criteria_for_bioretention

Mullane, J.M., Flury, M., Iqbal, H., Freeze, P.M., Hinman, C., Cogger, C.G., Shi, Z. 2015. Intermittent rainstorms cause pulses of nitrogen, phosphorus, and copper in leachate from compost in bioretention systems. Sci. Total Environ., 537, 294-303.

Muthanna, T.M., Viklander, M., Thorolfsson, S.T., 2008. Seasonal climatic effects on the hydrology of a rain garden. Hydrol. Processes 22(11), 1640-1649.

National Oceanic and Atmospheric Administration (NOAA), 2015. NOAA Atlas 14 point precipitation frequency estimates, Ohio. Hydrometeorological Design Studies Center, Precipitation Frequency Data Server. Available: http://dipper.nws.noaa.gov/hdsc/pfds/pfds_map_cont.html?bkmrk=oh

Ohio Department of Natural Resources (ODNR), Division of Soil and Water Conservation, 2006. Rainwater and land development: Ohio's standards for stormwater management, low impact development, and urban stream protection. 3rd edition. Ed: John Mathews.

Olson, N.C., Gulliver, J.S., Nieber, J.L., M. Kayhanian., 2013. Remediation to improve infiltration into compact soils. J. Environ. Manage. 117,85–95.

Page, J.L., Winston, R.J., Mayes, D.B., Perrin, C., Hunt, W.F. 2015a. Hydrologic mitigation of impervious cover in the municipal right-of-way through innovative stormwater control measures. J. Hydrol. 527, 923-932.

Page, J.L., Winston, R.J., Hunt, W.F. 2015b. Soils beneath suspended pavements: An opportunity for stormwater control and treatment. Ecol. Eng. 82, 40-48.

Palhegyi, G.E., 2009. Designing storm-water controls to promote sustainable ecosystems: science and application. J. Hydrol. Eng. 15(6), 504-511.

Passeport, E., Hunt, W.F., Line, D.E., Smith, R.A., Brown, R.A., 2009. Field study of the ability of two grassed bioretention basins to reduce storm-water runoff pollution. J. Irrig. Drain. Eng. 135(4), 505-510.

Piechota, T.C., Chiew, F.H., Dracup, J.A., McMahon, T.A., 2001. Development of exceedance probability streamflow forecast. J. Hydrol. Eng. 6(1), 20-28.

Pitt, R., Chen, S.E., Clark, S.E., Swenson, J., Ong, C.K., 2008. Compaction's impacts on urban storm-water infiltration. J. Irrig. Drain. Eng. 134(5), 652-658.

Pomeroy, C.A., Postel, N.A., O'Neill, P.A., Roesner, L.A., 2008. Development of storm-water management design criteria to maintain geomorphic stability in Kansas City metropolitan area streams. J. Irrig. Drain. Eng. 134(5), 562-566.

Prince George's County, Maryland (PGC)., 2001. The bioretention manual. Programs and Planning Division, Department of Environmental Resources.

Reynolds, W.D., Elrick, D.E., Youngs, E.G., Amoozegar, A., 2002. Ring or cylinder infiltrometers (vadose zone)." Methods of Soil Analysis - Part 4: Physical Methods, J.H. Dane and G.C. Topp, eds., Soil Science Society of America. Madison, WI.

Roesner, L.A., Bledsoe, B.P., Brashear, R.W., 2001. Are best-management-practice criteria really environmentally friendly? J. Water Res. Plann. Manage. 127(3), 150-154.

Sansalone, J.J., Teng, Z., 2004. In situ partial exfiltration of rainfall runoff. I: Quality and quantity attenuation. J. Environ. Eng. 130(9), 990–1007.

Schlea, D., Martin, J.F., Ward, A.D., Brown, L.C., Suter, S.A., 2014. Performance and Water Table Responses of Retrofit Rain Gardens. J. Hydrol. Eng. 19(8), 05014002.

Schueler, T.R., Fraley-McNeal, L., Cappiella, K., 2009. Is impervious cover still important? Review of recent research. J. Hydrol. Eng. 14(4), 309–315.

Smolek, A.P.*, Winston, R.J.*, Dorsey, J.D., Hunt, W.F., 2015. Modeling the hydrologic performance of bioretention and permeable pavement stormwater controls in northern Ohio using DRAINMOD: Calibration, validation, sensitivity analysis, and future climate scenarios. Final report submitted to the University of New Hampshire and the Chagrin River Watershed Partners. In fulfilment of NOAA Award number NA09NOS4190153. *These authors contributed equally to this work.

Soil Survey Staff, Natural Resources Conservation Service, United States Department of Agriculture, 2015. Web Soil Survey. http://websoilsurvey.nrcs.usda.gov/. Accessed 28 January 2015.

Tillinghast, E.D., Hunt, W.F., Jennings, G.D., 2011. Stormwater control measure (SCM) design standards to limit stream erosion for Piedmont North Carolina. J. Hydrol. 411(3), 185-196.

Tillinghast, E.D., Hunt, W.F., Jennings, G.D., and D'Arconte, P., 2012. Increasing stream geomorphic stability using storm water control measures in a densely urbanized watershed. J. Hydrol. Eng. 17(12), 1381-1388.

Tyner, J.S., Wright, W.C., Dobbs, P.A., 2009. Increasing exfiltration from pervious concrete and temperature monitoring. J. Environ. Manage. 90(8), 2636-2641.

United States Department of Agriculture, Natural Resources Conservation Service (USDA-NRCS), 1986. Urban hydrology for small watersheds. Technical Release 55 (TR-55). 2nd edition. United States Department of Agriculture (USDA), Natural Resources Conservation Service, Conservation Engineering Division.

United States Department of Agriculture, Natural Resources Conservation Service (USDA-NRCS), 2007a. Estimation of Direct Runoff from Storm Rainfall. Part 630, Chapter 10, National Engineering Handbook. Natural Resources Conservation Service.

United States Department of Agriculture, Natural Resources Conservation Service (USDA-NRCS), 2007b. Hydrologic Soil Groups. Part 630, Chapter 7, National Engineering Handbook. Natural Resources Conservation Service.

United States Environmental Protection Agency (USEPA), 2007. Reducing storm-water costs through low impact development strategies and practices. Rep. No. EPA 841-F-07-006, EPA, Washington, D.C. www.epa.gov/nps/lid. Accessed Feb 2012.

United States Environmental Protection Agency (USEPA), 2015. Storm water management model reference manual: Volume 1 – Hydrology. Office of Research and Development, Water Supply and Water Resources Division. EPA/600/R-15/162.

Vaughn, P.J., Trout, T.J., and Ayars, J.E. 2007. A processing method for weighing lysimeter data and comparison to micrometeorological ETo predictions. Agric. Water Manage. 88, 141-146.

Wadzuk, B.M., Hickman Jr, J.M., Traver, R.G., 2014. Understanding the role of evapotranspiration in bioretention: Mesocosm study. J. Sustainable Water Built Environ. 1(2), 04014002.

Walsh, C.J., Fletcher, T.D., Ladson, A.R., 2009. Retention capacity: a metric to link stream ecology and storm-water management. J. Hydrol. Eng. 14(4), 399-406.

Walsh, C.J., Fletcher, T.D., Burns, M.J., 2012. Urban Stormwater Runoff: A New Class of Environmental Flow Problem. PLoS ONE. 7(9): e45814. doi:10.1371/journal.pone.0045814.

Wang, L., Lyons, J., Kanehl, P., Bannerman, R., 2001. Impacts of urbanization on stream habitat and fish across multiple spatial scales. J. Environ. Plann. Manage. 28(2), 255–266.

Wardynski, B.J., Hunt, W.F., 2012. Are bioretention cells being installed per design standards in North Carolina? A field study. J. Environ. Eng. 138(12), 1210-1217.

Wardynski, B.J., Winston, R.J., Hunt, W.F., 2012. Internal water storage enhances exfiltration and thermal load reduction from permeable pavement in the North Carolina mountains. J. Environ. Eng. 139(2), 187-195.

Winston, R.J., 2016. Resilience of Green Infrastructure under Extreme Conditions. Dissertation, North Carolina State University. Raleigh.

Winston, R.J., Dorsey, J.D. Hunt, W.F., 2015. Monitoring the performance of bioretention and permeable pavement stormwater controls in Northern Ohio: Hydrology, water quality, and maintenance needs. Final Report Submitted to the University of New Hampshire and the Chagrin River Watershed Partners. In Fulfilment of NOAA Award number NA09NOS4190153. Available: http://www.crwp.org/files/OH_StormwaterControls_MonitoringReport2015.pdf

Winston, R.J., Dorsey, J.D., Smolek, A.P., Hunt, W.F., Submitted. Quantifying volume reduction and peak flow mitigation for permeable pavements in clay soils in northern Ohio. Submitted to Water Resour. Manage.

Winston, R.J., Smolek, A.P., Dorsey, J.D., Hunt, W.F., Submitted. Modeling the hydrologic performance of bioretention stormwater controls in northern Ohio using DRAINMOD: Calibration, validation, and sensitivity analysis. J. Hydrol.

Bioretention hydrology examined at three field sites

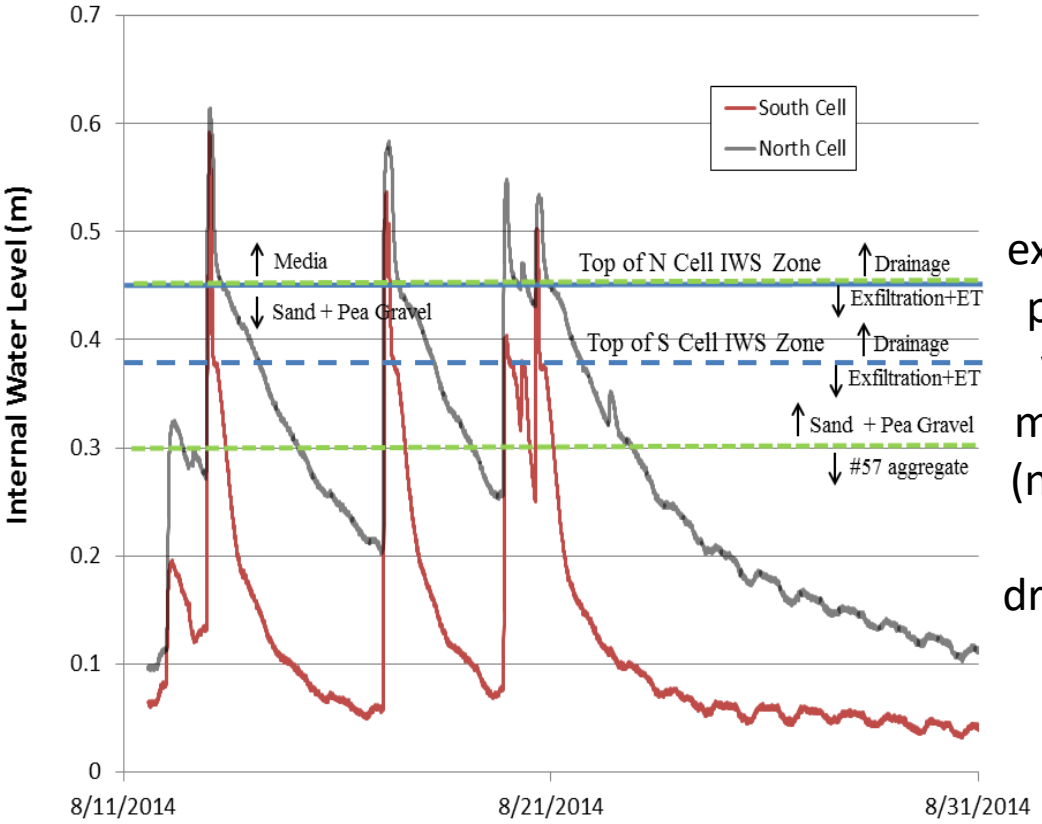

Lateral exfiltration provided volume mitigation (note non-linear drawdown)

Long-term hydrology (% of water balance)

Cell	Drainage	Overflow	Exfiltration/ET
UC	33.2	7.6	59.2
HA South	51.1	6.8	42.1
HA North	57.2	6.9	36.0

Bioretention performance influenced by underlying soils, IWS zone configuration, and bowl storage